NASA TECHNICAL NOTE

NASA TN D-7425

NASA TN D-7425

TWO-DIMENSIONAL ANALYTICAL AND EXPERIMENTAL PERFORMANCE COMPARISON FOR A COMPRESSOR STATOR SECTION WITH D-FACTOR OF 0.47

by Nelson L. Sanger

Lewis Research Center
Cleveland, Ohio 44135

NATIONAL AERONAUTICS AND SPACE ADMINISTRATION • WASHINGTON, D. C. • OCTOBER 1973

1. Report No.	2. Government Accession No.	3. Recipient's Catalog No.
NASA TN D-7425		

4. Title and Subtitle	5. Report Date
TWO-DIMENSIONAL ANALYTICAL AND EXPERIMENTAL PERFORMANCE COMPARISON FOR A COMPRESSOR STATOR SECTION WITH D-FACTOR OF 0.47	October 1973
	6. Performing Organization Code

7. Author(s)	8. Performing Organization Report No.
Nelson L. Sanger	E-7280
	10. Work Unit No. 501-24
9. Performing Organization Name and Address	11. Contract or Grant No.
Lewis Research Center National Aeronautics and Space Administration Cleveland, Ohio 44135	
	13. Type of Report and Period Covered
12. Sponsoring Agency Name and Address	Technical Note
National Aeronautics and Space Administration Washington, D.C. 20546	14. Sponsoring Agency Code

15. Supplementary Notes

16. Abstract

Analytically computed flow parameters were compared to measured values for the midspan double-circular-arc section of a stator in subsonic flow. Analytical procedures included calculations for inviscid flow, blade surface boundary layers, and loss coefficients. Comparisons were made at three incidence angles. Methods for prescribing the exit fluid angle in inviscid flow calculations were investigated. Measured loss coefficients were compared to calculated values. Two methods for predicting performance involving iterative use of ideal flow and boundary layer calculations were investigated.

17. Key Words (Suggested by Author(s))	18. Distribution Statement
Compressors Turbomachinery Airfoil aerodynamics Stator blades	Unclassified - unlimited

19. Security Classif. (of this report)	20. Security Classif. (of this page)	21. No. of Pages	22. Price*
Unclassified	Unclassified	40	Domestic, $3.00 Foreign, $5.50

* For sale by the National Technical Information Service, Springfield, Virginia 22151

CONTENTS

TWO-DIMENSIONAL ANALYTICAL AND EXPERIMENTAL PERFORMANCE COMPARISON FOR A COMPRESSOR STATOR SECTION WITH D-FACTOR OF 0.47

by Nelson L. Sanger

Lewis Research Center

SUMMARY

Analytically computed flow parameters for the midspan, double-circular-arc blade section of a highly loaded compressor stator have been compared with measured flow parameters. Analytical calculations were performed for inviscid flow on a blade-to-blade flow plane, boundary layer on the blade suction and pressure surfaces, and total pressure loss coefficient. All velocities were subsonic. Comparisons were made at three incidence angles.

Inviscid flow calculations require the outlet flow angle as input. Thus, either some trailing edge condition must be specified and the resulting exit angle accepted, or an exit angle may be specified and the resulting flow distribution accepted. For one method, iterations were performed on the exit angle until suction and pressure surface pressures were equal at the trailing edge. With this method, surface pressures diverged from measured values near the trailing edge, and exit angles differed by as much as 10^{o} from measured values. A second method used measured values of exit angle as input to the inviscid flow calculations. Surface pressures showed much better agreement; pressures on suction and pressure surface became equal at between 91.5 and 92.5 percent chord for all incidence angles.

Boundary layers were calculated as being turbulent from near the leading edge. Losses were calculated using a flow model developed by Speidel which includes a term to account for losses due to separation. To bring calculated losses into agreement with measured losses, very large boundary layer initial thicknesses were necessary. This indicated a need for further study of the calculation procedure to determine its general applicability.

Inviscid flow and boundary layer calculations were combined iteratively to attempt to account for real flow effects. An existing method was extended to apply to cases with boundary layer separation. A second method was investigated which entailed adding a calculated boundary layer displacement thickness to the original blade profile to obtain a new effective blade profile before recalculating the inviscid flow. The former method was judged more accurate and less cumbersome to apply.

INTRODUCTION

The real flow through a compressor blade row is compressible, unsteady, three-dimensional, highly viscous in certain regions, and may contain both subsonic and supersonic flow regions. With the advent of large computers, the ability to analytically describe real flow phenomena has been greatly advanced. But it is still impossible, for analytical and computer storage reasons, to adequately analyze real compressor flow with a single program. However, by making certain simplifying assumptions, such as flows that are steady and two-dimensional, with viscous effects confined to a boundary layer, the analytical procedure can be divided into separate segments. The results of individual calculation procedures can then be combined (e.g., a two-dimensional inviscid flow calculation and a blade surface boundary layer calculation), and approximations to the real flow can be made. How closely the computed results approach the real flows must be ascertained from comparisons between computed and experimental data. If an iterative procedure is required, the degree of accuracy obtained at each stage of the computation will determine how many successive applications of the calculation procedure are necessary, thereby providing a measure of the compromise between accuracy and cost. The term cost is used in a qualitative sense to indicate the number of calculation cycles and amount of user effort required to effect a solution. The results of comparisons between analysis and experiment will also provide a means for altering and improving the analytical procedures.

This report presents a comparison of computed and measured flow parameters for a highly loaded compressor stator blade section. The objective is to develop and evaluate several methods for prescribing input boundary conditions to existing analytical methods to enable accurate predictions of blade performance to be obtained. The meaured data were obtained from a conventionally designed solid stator blade (ref. 1). The midspan section of the blade, where flow would be expected to approximate two-dimensionality, was selected for consideration. All flow velocities were subsonic. The data included inlet and outlet station flow properties, blade surface pressures, and total pressure loss coefficients obtained from detailed wake surveys.

The computed results were obtained by using a compressible inviscid flow calculation on the blade-to-blade flow plane (ref. 2), a boundary layer method which calculates laminar and turbulent compressible boundary layers by integral techniques (ref. 3), and a loss calculation which computes loss coefficient using Speidel's method (ref. 4). Of particular interest are the calculated loss coefficients and outlet flow angles. Also discussed are some problem areas related to the application of these calculation procedures.

ANALYTICAL TECHNIQUES

This section describes the analytical procedures used in the study and some problem areas encountered in applying them. An inviscid flow calculation on the blade-to-blade flow plane provides velocities and flow angles. Blade surface velocities from the ideal flow calculation are used to compute boundary layer growth. Loss parameters are calculated using information from both the inviscid flow and boundary layer calculations.

Inviscid Flow Calculations

The equation in the inviscid flow program (ref. 2) which describes the flow in the blade-to-blade flow plane is an elliptical partial differential equation for the stream function. The inviscid flow program (ref. 2) solves this equation for the subsonic, compressible flow regime. It is necessary to specify as input the fluid properties, inlet total temperature and density, weight flow, blade geometry, inlet and outlet flow angles, and the finite difference mesh. As output the program provides blade surface velocities, velocities and flow angles at all internal mesh points, and streamline coordinates and directions.

Because the nature of the equations dictates that the solution be of the boundary value type, certain variables must be specified on the downstream boundary. In this program the outlet flow angle must be specified. This is one of the unknowns of principal interest in the compressor design process. Consequently, an additional aspect of the inviscid flow problem is to determine a criterion for setting outlet flow angle, probably one related to calculated flow conditions in the trailing edge region.

Historically, inviscid flow programs were first applied to wing sections which had sharp or cusped trailing edges. The downstream boundary condition was specified such that the stagnation point was located on the sharp trailing edge in order to avoid the mathematical condition of infinite velocities around the trailing edge. Differences between calculated and measured flow behavior were ascribed to viscous effects.

Compressor blade profiles, which generally have rounded trailing edges, cannot be analyzed in the same manner because there is no way to know the location of the stagnation point. One method of specifying the downstream boundary condition that has been used is analogous to the original wing methods. With this method an attempt is made to minimize the velocity differences between suction and pressure surface at the trailing edge (analogous to avoiding the infinite velocity condition). This method was used initially in the present study. To apply it, the inviscid flow calculation is performed several times, each for a different value of outlet angle. The solution is chosen for which the pressures (or velocities) on the suction and pressure surfaces are equal at the blade trailing edge. Normally, several iterations are required to find the exit angle that satis-

fies the closure requirement. The flow condition corresponding to closure is treated as a base or reference condition.

Boundary Layer Calculations

The blade surface velocities from the inviscid flow program are used to calculate the boundary layer growth using the program of reference 3. In addition to the surface velocities, required input includes upstream flow conditions, fluid properties, blade surface geometry, and, in some cases, initial boundary layer thicknesses. Among the output provided by the program are the conventional boundary layer thicknesses, form factors, wall friction coefficient, and momentum thickness Reynolds number.

The program uses integral methods to solve the two-dimensional compressible laminar and turbulent boundary layer equations in an arbitrary pressure gradient. Cohen and Reshotko's method (ref. 5) is used for the laminar boundary layer, transition is predicted by the Schlichting-Ulrich-Granville method (ref. 6), and Sasman and Cresci's method (ref. 7) is used for the turbulent boundary layer.

A boundary layer which is initially laminar may proceed through normal transition to a turbulent boundary layer, or it may undergo some form of laminar separation before becoming turbulent. To provide flexibility for analyzing this behavior, several program options (discussed subsequently) are available to the user, some of which were used in the present study. The calculations may proceed from a laminar boundary layer through transition to turbulent calculations. However, if laminar separation is predicted before transition, the turbulent calculations may be started by specifying a factor (C_θ) by which the last calculated value of momentum thickness is multiplied. This new momentum thickness and a value for form factor based on the last calculated momentum thickness Reynolds number are used as initial values for the turbulent calculations. Another option permits the user to force transition from laminar to turbulent boundary layer at any station specified by the user, provided that transition or laminar separation have not already occurred before that station. Another option permits the user to begin turbulent calculations at any station by specifying the initial values for displacement and momentum thickness.

Boundary layer development over compressor blades is a subject that is not yet clearly understood. Although the boundary layer on each surface begins as laminar from the stagnation point, the extent of laminar flow before either laminar separation or normal transition occurs is not readily determined. Some factors which influence laminar boundary layer growth and separation on stationary blades are surface pressure gradient, turbulence level, Reynolds number, surface roughness, and, to some extent, the degree of three-dimensional flow. It is not often that all of these factors are measured in experimental compressor tests. Consequently, there is a lack of clear, authoritative in-

formation. Furthermore, because most of the attention given to compressor blade boundary layer flow is given to the suction surface boundary layer, very little is presently known about the development of pressure surface boundary layers.

The methods used to calculate compressor boundary layer flow have commonly assumed the boundary layer becomes turbulent at the beginning of an adverse pressure gradient, or, because of the turbulent compressor flow environment, it becomes turbulent very near the blade leading edge (ref. 8). In either case, the initial turbulent boundary layer conditions must be specified, and this information is not known with certainty. Although the assumption of early transition to turbulent boundary layer may be correct for many, or even most compressor applications, experimental evidence has recently been presented by Walker (ref. 9) which shows that laminar boundary layers can persist for long distances on actual compressor stator blading (as distinguished from cascade tests).

Consequently, in the present study, boundary layers were calculated as being initially laminar from the leading edge region on both blade surfaces. A discussion of the results, and of the subsequent steps taken, are presented in the RESULTS AND DISCUSSION section.

Once a turbulent boundary layer has been established, a criterion must be established for indicating turbulent separation. Sandborn and Liu (ref. 10) have referred to turbulent boundary layer separation as "one of the most important unsolved problems in fluid mechanics," and the Stanford Conference Evaluation Committee (ref. 11) concluded that no boundary layer calculation method then in use (1968) was mathematically or physically legitimate in the separation region, and that data against which to compare analytical methods were equally suspect. It is therefore clear that any turbulent separation criterion will be approximate and the results must be interpreted accordingly.

A separation criterion common to compressor blade analyses which use integral boundary layer methods is the incompressible form factor H_i. Values of 1.8 to 2.6 have been proposed and used in the past (e.g., von Doenhoff and Tetervin, ref. 12). Experience by the author with the boundary layer method of reference 3 on several blade shapes has shown a trend for rapid calculated boundary layer growth once H_i has reached 2.0. This indicates that choices of H_i greater than 2.0 will not appreciably alter the location of separation. In addition, it is likely that the equations lose validity in regions of high H_i, corresponding to separated flow. Therefore, a value of $H_i = 2.0$ was selected to signal turbulent boundary layer separation. This criterion will provide, at best, a consistent engineering estimate of the location of turbulent separation and an approximation of the corresponding boundary layer thicknesses at that location. Although the experimental data are limited, an attempt will be made in the RESULTS AND DISCUSSION section to assess the accuracy of this criterion.

Loss Calculations

Various investigators have developed models for calculating total pressure loss coefficient based on boundary layer parameters and flow properties at the trailing edge of a blade. Lieblein's incompressible flow analysis (ref. 13) and Stewart's compressible analysis (ref. 14) were accomplished for the case of a boundary layer which remained stable to the trailing edge. If boundary layer separation was indicated, an estimate of the loss could be obtained only by extrapolating the respective boundary layer thicknesses to the trailing edge station. Achieving good agreement with experimentally measured values of loss coefficient using this procedure would seem quite unlikely.

Because the calculation of turbulent boundary layer separation is not exact, the prospects for calculating loss in a separated region are not encouraging. For the present, such ventures must be regarded as approximate. Speidel (ref. 4) performed a one-dimensional analysis and obtained an expression for the loss due to separation. This was incorporated into an expression for overall loss coefficient which closely resembles Lieblein's expression. Speidel and Schlichting report good agreement of the expression with experimental data (refs. 4 and 8). The method was used in the present study. Because reference 4 is in German, the method is developed in appendix B.

Iterative Use of Calculation Procedures

The goal of approximating real flow by separately calculating the ideal flow and the boundary layer development presumably can be achieved through a series of successive applications of each calculation procedure. For example, the inviscid flow calculation will provide the surface velocities for a boundary layer calculation. The boundary layer calculation will provide boundary layer parameters and input for a loss coefficient calculation. Cross-interpretation of the separate calculations may lead to refinements and recalculation of individual programs with an aim to converge on a solution which closely approximates real flow.

It is apparent that each individual calculation has an effect on the succeeding one, and that several cycles through the series of calculation procedures may be involved. This can become expensive, both in computer time and user effort, particularly for broad analytical studies in which many blade sections and blade rows are involved. Some compromise must, therefore, be affected between accuracy and cost. Consequently, in evaluating the effectiveness of the methods employed, consideration will be given not only to accuracy but also to the number of calculation cycles and amount of user effort required.

EXPERIMENTAL BLADE

The measured data used in this report were obtained from the midsection of a conventional solid stator used in the baseline stage of reference 1. The design of this stator is completely described in reference 15 and the profile geometry is shown in figure 1. The stator was designed to be representative of the middle stages of a compressor. A cross section of the flow path is shown in figure 2. The lack of flow path curvature is evident. A double-circular-arc airfoil shape was used. Design equations from reference 16 were used to set camber, incidence, and deviation. A summary of geometrical and aerodynamic design data is given in table I. The measured loss against incidence angle curve of the midspan section is shown in figure 3 as an example of the performance.

TABLE I. - SUMMARY OF DESIGN PARAMETERS

50-PERCENT SPAN FROM TIP

Total chamber, φ_T, deg	54.35
Total chord, C_T, cm	5.96
Maximum thickness to chord ratio, T_{max}/C_T	0.09
Setting angle, γ, deg	15.06
Solidity, σ	1.35
Inlet Mach number, M_1	0.57
Diffusion factor, D	0.47
Incidence angle (to mean line), i, deg	-2.23
Deviation angle, δ, deg	12.12
Loss coefficient, $\overline{\omega}$	0.071
Inlet velocity, V_1, m/sec	194.5
Inlet axial velocity, $V_{z,1}$, m/sec	149.0
Inlet relative angle, β_1', deg	40.0
Outlet velocity (axial), V_2, $V_{2,z}$, m/sec	150.4

RESULTS AND DISCUSSION

In this section the computed and experimentally measured results are compared. Measured data represent real flow, and efforts are directed toward determining what modifications and/or specific inputs to the analytical methods are necessary to produce agreement with measured data. The flow parameters to be compared are the blade surface pressure coefficients, loss coefficient, and outlet flow angle.

The results are presented and discussed in the sequential order in which the computed solutions must be obtained: inviscid flow, boundary layer, and loss calculations. In a final section the foregoing results are evaluated and some iterative procedures are synthesized.

Inviscid Flow Calculations

Three conditions were chosen for detailed analytical investigation: the design point ($i = -2.4^{\circ}$) and conditions having both higher and lower than design incidence angle ($i = 0.3^{\circ}$ and $i = -6.6^{\circ}$). These conditions are indicated as solid circles in figure 3, which shows the operating points at which experimental data were taken.

The blade surface pressure distributions are shown in figure 4 for both the experimental and calculated cases. As shown in figure 4, it is assumed for the calculated case that pressures on the pressure and suction surfaces become equal at the blade trailing edge. The calculations compare favorably with experiment over the front portion of the blade, but discrepancies become greater toward the trailing edge. In addition, a comparison of the computed and measured exit flow angles (fig. 4) reveals considerable differences. It was found that to close the analytical surface pressure distributions at the trailing edge the analysis required 8° to 10° more fluid turning than was measured.

The differences between measured and calculated results are believed to be due to three principal effects. One effect is produced by the uncertainty of the downstream boundary condition (placement of stagnation condition on a rounded trailing edge). The second effect is that produced by boundary layer blockage and separation. The suction surface separation is indicated experimentally for $i = -2.4^{\circ}$ and $i = 0.3^{\circ}$ by the flattening of the pressure distribution near the trailing edge region. The third effect is the degree of three-dimensional flow actually present in the measured data. At the 50-percent span location there should be a minimum amount of radial flow. There will be some radial flow present, however, and it will affect the comparison with calculated flows. It is not possible to quantify any of the three aforementioned effects.

The inviscid flow calculations were repeated using as input the measured values of fluid exit angle and observing the associated trailing edge flow condition. The calculated surface pressure coefficients are shown in figure 5 and two general results should be noted. First, using the experimental exit angle in the calculations results in a closer comparison between experimental and calculated surface pressures, particularly from the 50-percent position rearward. Second, using the experimental exit angle resulted in the crossing of the computed surface pressure distributions upstream of the trailing edge. In fact, the distributions for all operating conditions crossed between 91.5 and 92.5 percent of axial chord. This suggests the possibility that a criterion for prescribing exit angle may be devised which is a function of the crossing point (among other pa-

rameters) of the surface pressure distributions. Methods for prescribing exit angle will be discussed in more detail later in this section.

Boundary Layer and Loss Calculations

No experimental boundary layer measurements were taken, thereby preventing direct confirmation of analytical boundary layer computations. However, experimental wake surveys were conducted. These permit comparisons of experimental and calculated loss coefficients, but they do not permit the source of any discrepancies to be identified.

The boundary layers were calculated as laminar on each blade surface beginning at the stagnation point. In every case, due to the magnitude of the pressure gradient, laminar separation was indicated before transition on both the suction and pressure surfaces. The calculations were then restarted from the indicated point of separation. To begin the turbulent boundary layer calculations the initial conditions used were the last calculated laminar values for momentum thickness and Reynolds number based on momentum thickness. A sample plot of incompressible form factor and displacement and momentum thicknesses for the design point condition is shown in figure 6.

The calculated loss coefficient corresponding to the boundary layer distribution shown in figure 6 was $\overline{\omega} = 0.017$. Loss calculations made at off-design conditions, for similar treatment of the boundary layer, showed little variation of $\overline{\omega}$ with incidence angle. The calculated loss coefficients are considerably lower than the experimental values of $\overline{\omega} = 0.054$ to 0.093 shown in figure 3.

An additional boundary layer calculation was made in which the boundary layer was initially laminar, and after laminar separation occurred the initial turbulent momentum thickness was a factor of five greater than the last calculated laminar momentum thickness before laminar separation. An increase in momentum thickness of this magnitude appears to be out of the range of reported boundary layer experience. Despite this, however, its effect on calculated loss coefficient was only to increase it to $\overline{\omega} = 0.037$.

Because the calculations for initially laminar boundary layers result in very large increases in boundary layer thickness through the separation-transition region, an alternative approach appears necessary. One such approach, as described earlier, is to assume the boundary layer to be turbulent from very near the leading edge on both blade surfaces as Schlichting (ref. 8) and others have done. This procedure was followed next. Some initial considerations must first be discussed, however.

When the boundary layer is assumed initially turbulent, what is implied is that the laminar boundary layer separates and reattaches almost immediately. The important unknowns in this problem then include initial turbulent displacement and momentum thicknesses. They must be determined by inference - that is, what values of initial displacement and momentum thickness produce agreement between measured and computed

loss coefficient? (Loss coefficient is a direct function of momentum thickness at the trailing edge, and, therefore, related to the initial value chosen at the leading edge, see eq. (B2).) This procedure implicitly assumes that the boundary layer and loss models are both valid, an assumption that cannot be proved at this time.

A further consideration which will affect the loss calculations is the relation between initial thicknesses chosen for the suction surface and those chosen for the pressure surface. Because the initial conditions occur in different pressure gradients on each surface, and because the gradients change with incidence angle, it is conceivable that different initial turbulent boundary layer thicknesses should be chosen for each surface. However, the testing of the large number of possible combinations, none of which are necessarily unique, would complicate and lengthen the computation process. Therefore, for the sake of simplicity the same initial displacement and momentum thickness used on the suction surface was used also on the pressure surface for any given calculation.

In choosing initial values, δ^* and θ were always chosen such that the initial ratio of δ^*/θ was 1.4. There are several precedents for this choice. Schlicting (ref. 6) reports that transition on a flat plate results in an initial turbulent form factor of 1.4. Gostelow (ref. 17) used an initial form factor of 1.4 in his analytical calculations for compressor blades in cascade. And McNally (ref. 3) found that on airfoil tests (ref. 18), natural transition was calculated, and the initial turbulent form factor was 1.4.

One final question relates to the effect of initial thickness on turbulent boundary layer separation prediction. Using the Speidel loss model, loss calculations depend on separation location (local surface velocity and blade profile thickness at the separation point are used) and on boundary layer parameters at separation. If different initial thicknesses were found to produce different separation locations, then it might be possible to find two or more initial thickness conditions which correspond to the same loss. To investigate this effect, a series of suction surface boundary layer calculations were made for the design incidence operating condition. A plot of incompressible form factor is given in figure 7 for four initial thicknesses ranging from 0.00609 to 0.0609 centimeter. Differences are seen over the early portion of the blade where form factor is not critical. But all curves show the same behavior over the latter portion of the blade where form factor rises sharply to separation values. The location of indicated separation shows little variation for the four initial thicknesses considered.

Analytical calculations were made for the three operating conditions previously noted ($i = -6.6^\circ$, -2.4°, and 0.3°). One additional operating point was considered for this set of calculations, the condition where $i = 2.88^\circ$ (see fig. 3). Boundary layer and loss calculations were performed for a range of initial thickness values until loss coefficients were brought into agreement with experimental values. The initial displacement and momentum thicknesses which produced this agreement at each incidence angle are given in table II. Plots of the calculated turbulent boundary layer distributions at each

TABLE II. - INITIAL BOUNDARY LAYER THICKNESSES AND

CORRESPONDING ANALYTICAL LOSS COEFFICIENTS

Incidence angle, i, deg	Initial displacement thickness, δ_i^*, cm	Initial momentum thickness, θ_i, cm	Analytical loss coefficient, $\overline{\omega}$	Experimental loss coefficient, $\overline{\omega}$
2.9	0.0914	0.0652	0.092	0.093
.3	.0685	.0490	.073	.072
-2.4	.0610	.0435	.064	.062
-6.6	.0426	.0345	.056	.055

incidence angle are presented in figure 8. Separation is indicated when the incompressible form factor curve intersects the line $H_i = 2.0$.

Two results should be noted. First, in order to predict the experimental loss coefficient at the design point, i = -2.4, it was necessary to begin the turbulent boundary layer calculations with an initial δ^* of 0.061 centimeter and an initial θ of 0.0435 centimeter. These are rather large values, corresponding to 1 and 0.7 percent of blade chord, respectively. The second point to be noted is that the initial boundary layer thicknesses increased as incidence angle increased.

Prediction of Turbulent Boundary Layer Separation

Since no experimental boundary layer measurements were taken, it was therefore not possible to establish the location of boundary layer separation accurately. The only measurements available are surface pressure distributions. The criterion that was used to locate separation was to note when this distribution changed slope and became flat. It was assumed that when separation occurred velocity deceleration ceased and static pressure remained constant. This will provide a gross estimate of the location only, since measurements to indicate streaking, velocity profile reversals, and shear stress distributions are not available.

To illustrate the process, refer to figure 4(a) in which a dashed line at constant C_p is drawn through the last experimental point on the suction surface. At the X/C_t location where this line intersects the faired curve through the nonseparated points (dashed line also), separation was inferred to occur.

This procedure is clear for the conditions shown in figures 4(a) and (b). However, in figure 4(c) (i = -6.6) suction surface separation is not clearly indicated. It was inferred to occur at the last experimental point ($X/C_t = 0.86$) by using the following process.

From the experimental data presented in figures 4(a) and (b), the difference in suction surface C_p from the inferred separation point to the minimum value is as follows:

(a) For $i = 0.3$, $\Delta C_p = 0.17 - (-0.5) = 0.67$

(b) For $i = -2.4$, $\Delta C_p = 0.13 - (-0.53) = 0.66$

In each case, this corresponds to a maximum surface velocity to velocity at separation of $V_{max}/V_{sep} = 1.33$. Although the last suction surface data point in figure 4(c) does not show evidence of flattening, the ΔC_p at that point is 0.69 and $V_{max}/V_{local} = 1.33$. Therefore, it was felt that there was adequate reason to use it as an indicated separation point.

Taking the axial chord locations thus determined, and going to the analytical boundary layer curves of H_i against percent axial chord (fig. 8), one can find the corresponding H_i values at separation. These are shown in table III. They are relatively close to the $H_i = 2.0$ values used in this study. Although this is a rather unrefined process, it does provide some justification for the use of $H_i = 2.0$ as a separation criterion. Additional data and more refined methods of evaluating experimental separation location will aid in determining the general applicability of this criterion.

TABLE III. - FORM FACTORS AT SEPARATION

Incidence angle, i, deg	Pressure coefficient rise, ΔC_p	Axial location of separation, X/C_t	H_i at separation (from fig. 7)
0.3	0.67	0.765	1.88
-2.4	.66	.815	1.88
-6.6	.69	.86	1.94

Iterative Applications of Inviscid and Viscous Calculations

In the foregoing sections the results obtained from once-through applications of the calculation procedures have been presented. In order to approximate real flow performance some refinements to the procedures are clearly necessary, and indeed, were anticipated. In this section some approaches involving iterative applications of the calculation procedures will be developed and discussed.

General observations. - Inviscid flow calculations presented thus far allow several conclusions. First, choosing an exit flow angle such that surface pressure distributions closed at the trailing edge predicted, as expected, much more fluid turning that was actually achieved. Also, surface pressures began to diverge from measured values as the trailing edge region was approached. Second, using the experimentally measured

exit angle in the analytical calculations resulted in good agreement between experimental and analytical surface pressures. It is instructive to know that if the exit flow angle can be approximated, the surface pressures resulting from a single pass through the inviscid flow calculations are in reasonable agreement with measured values. The search then becomes centered on methods for approximating exit flow angle. In this regard, it is of interest to note that in the calculations using measured exit angle (fig. 5) all of the analytical surface pressure distributions showed crossing between 91.5 and 92.5 percent of axial chord.

This therefore suggests that one possible approach may be to construct a relation between the position of crossing of the surface pressure distributions (and thereby, the exit angle that produced it) and the pressure gradient or other aerodynamic parameters which are available from the inviscid flow calculations. The correlation with aerodynamic parameters available from the inviscid flow calculations would be desirable in order to avoid complex empirical relations relating blade shape, thickness distribution, solidity, camber, and other geometric parameters. If such a relation could be constructed, it would permit the exit angle to be determined from application only of the inviscid flow calculation thereby reducing analytical complexity and cost. However, the synthesis of such a relation requires additional data from blades of widely differing designs.

Gostelow method extended. - Gostelow (ref. 17) was successful in approximating real flow by using only an inviscid flow calculation. However, he investigated relatively lightly loaded blades (C4 profile with 30° camber) in low subsonic flow. He predicted exit flow angle and surface pressure distributions quite closely using the Martensen inviscid flow method and a "fairing-in" process near the trailing edge of the blade.

The "fairing-in" process is an empirical method and constitutes an approximation for viscous and rounded trailing-edge effects. Several inviscid flow calculations are made, and a tangent to the C_p distributions is faired in at the 85-percent chord location on each surface (see fig. 9). The "correct" solution (exit angle condition) is the one for which the faired-in tangents just meet at the trailing edge (100-percent chord). Gostelow followed Preston's analysis (ref. 19) which asserts that no net vorticity is discharged into the wake and that wake curvature effects may be neglected. The 85-percent chord location was chosen on the basis of work reported by Spence and Beasley (ref. 20).

It should also be noted that, in most cases, for the condition corresponding to the faired-in tangents meeting at the trailing edge, the calculated surface pressure curves will cross inside the trailing edge. This agrees with the results obtained from calculations in this study, as noted in the previous section.

In the examples shown in reference 17 the suction surface boundary layer was well behaved, showing no evidence of separation. It seems unlikely that the method can be applied directly to the data evaluated in this report because separation is indicated over roughly the last 20 percent of the suction surface. Indeed, an application of the refer-

ence 17 method to the plots of figure 5, where measured exit angles were used as input, showed the tangents to cross at axial chord locations between 93 and 94 percent rather than 100 percent. Thus, a direct application of Gostelow's method would have overestimated the fluid turning in these cases.

A method has been devised for modifying this general approach to permit application to blades having separated boundary layers. In brief, the method applies the tangent criterion at the indicated separation point when it occurs upstream of the 85-percent chord position. More specifically, the method requires iterative use of the inviscid flow and boundary layer calculations and is now outlined:

(1) Perform an inviscid flow calculation iteratively to determine the case for which suction and pressure surface C_p curves cross at trailing edge (base condition).

(2) Calculate the boundary layer assuming it to be turbulent from near the leading edge.

(3) Determine the location of predicted boundary layer separation using $H_i = 2.0$.

(4) From the C_p against X/C_t distribution for the base condition, determine the C_p at the separation location. Subtract the minimum C_p from it to get the ΔC_p that produced separation.

(5) Recalculate the inviscid flow at some $\beta_2' > \beta_{2base}'$ (e.g., $\beta_2' - \beta_{2base}' \cong 5^o$).

(6) Add ΔC_p to the minimum C_p to locate the new C_p corresponding to separation and from which the tangent is to be faired in. Fair in the tangent from this point.

(7) Fair in the tangent on the pressure surface C_p curve from the $X/C_t = 0.85$ point.

(8) Repeat steps (5) to (7) until the faired-in curves cross at the trailing edge ($X/C_t = 1.0$). The exit flow angle corresponding to this final calculation is the approximation to the real flow angle.

The tangent to the suction surface C_p is faired in from the point of estimated separation. If ΔC_p is used as the parameter in steps (4) and (6) the pressure which corresponds to separation in the first iteration is transferred to subsequent iterations. Repeated applications of the boundary layer calculation are therefore avoided. The X/C_t was not used as the separation-determining parameter because the point at which separation occurs is largely a function of pressure rise (i.e., ΔC_p) rather than distance.

The previously discussed compressor stator data are used to check the method. Steps (1) to (3) have already been performed (figs. 4 and 8). The series of iterations outlined in steps (5) and (8) are not carried out, however. Instead the calculations performed using experimentally measured exit angle (fig. 5) are used. This calculation represents the "correct" condition and if fairing in from the appropriate position results in crossing at $X/C_t = 1.0$ the method outlined previously is confirmed.

The boundary layer curves of figure 8 can be used to find the location of suction surface separation (using $H_i = 2.0$). From the inviscid flow calculations (fig. 4) at those X/C_t locations the C_p at separation and the rise in C_p from minimum can be deter-

TABLE IV. - DETERMINATION OF

PRESSURE RISE TO SEPARATION

FOR FIRST ITERATION

Incidence angle, i, deg	Suction surface		
	$(X/C_t)_{sep}$	$(C_p)_{sep}$	ΔC_p
0.3	0.785	0.07	0.66
-2.4	.83	.06	.66
-6.6	.865	.05	.65

mined (ΔC_p). These are given in table IV.

The ΔC_p values thus determined are applied to the suction surface of the inviscid flow calculation of figure 5 as shown in figure 10. Tangents are faired-in from the respective suction surface points and from the point on the pressure surface corresponding to $X/C_t = 0.85$. The faired-in curves intersect at just under the $X/C_t = 1.0$ position, indicating that the exit angles used in the calculation (which were the experimentally measured angles) were very close to what would have been determined by direct application of the modified Gostelow method. The locations of the intersections of the faired-in tangents as determined from figure 10 are as follows:

Incidence angle, i, deg	Location of intersection of tangents, X/C_t
0.3	0.99
-2.4	.99
-6.6	.98

Therefore, the modified Gostelow method produced an accurate result, at least for the set of data evaluated. This approach involves several iterations of the inviscid flow calculation and a single pass through the boundary layer calculation. One area of uncertainty is the choice of initial boundary layer thickness. It was shown earlier (fig. 7) that for a typical surface pressure distribution the predicted location of separation was not sensitive to initial thickness. The user therefore has some latitude in the choice of

initial δ^*. Once δ^* is specified, an initial form factor of 1.4 is appropriate and will then specify momentum thickness.

Displacement-thickness-added method. - The method just described approximates the effect of the boundary layer by altering the inviscid flow surface pressure distribution. Another method for approximating the effect of boundary layer is to add calculated boundary layer displacement thickness to the blade profile geometry and recalculate the inviscid flow over the redefined blade. The process can be repeated until convergence within desired limits is achieved. An outline of the procedure is as follows:

(1) Perform the inviscid flow calculation iteratively to determine the case for which suction and pressure surface C_p curves cross at the trailing edge (base condition or ideal condition).

(2) Calculate the boundary layer, assuming it to be turbulent from the leading edge.

(3) Add the boundary layer displacement thickness to the original blade profile, thus defining a new effective blade profile.

(4) Recalculate the inviscid flow for the new effective profile.

(5) Repeat steps (2) to (4) until inviscid flow results converge within acceptable limits.

This procedure was carried out for the design point (i = -2.4). The inviscid flow calculation shown in figure 4(b) constitutes the base condition (step (1)). The boundary layer calculation corresponding to it, shown in figure 8(b) (initial displacement thickness on both surfaces, 0.061 cm), constitutes step (2). The calculated displacement thickness was added to the blade profile geometry. Since boundary layer separation was indicated on the suction surface, the new profile was extrapolated from the separation point to the trailing edge to continue a smooth profile shape. The inviscid flow calculation requires geometry with a trailing edge radius, so the profile was closed with a circular arc. The resulting blade section profile is shown in figure 11.

The pressure distribution calculated by the inviscid flow program is shown in figure 12. The local accelerations near the trailing edge are caused by the large trailing edge radius. Because of the local accelerations it was necessary to devise a method for setting exit angle which was not dependent on the calculated surface pressures. In the approach used, it was assumed that the flow follows the direction of the effective profile (original geometry plus boundary layer displacement thickness) to the point at which the trailing edge circle joins the profile. The downstream angle is then taken to be an average of the two surface angles at the respective points of tangency with the trailing edge circle. This procedure neglects three-dimensional effects and assumes complete mixing to a uniform downstream angle. If separation is predicted (as it was in this case), fluid turning is assumed to cease at the predicted separation point and the surface angle there is used in the average. The surface angles of the new effective blade are directly available from the spline fits in inviscid flow calculations.

It is clear from the results that because of the large boundary layer thickness and separation the method did not converge in this case. In this, and similar cases, one pass through the calculation procedure is probably sufficient.

In general, this method should converge. The reason it did not in this case is that the initial boundary layer thickness was chosen in order to match calculated loss with measured loss.

The exit angle obtained by this procedure was -1.25° compared to 1.6° measured experimentally. The surface pressure distributions obtained (fig. 12) show very good agreement with surface pressure data on the pressure surface. Although the predicted pressures on the suction surface are displaced from the data somewhat, agreement is acceptable.

Exit condition adjusted for separation. - One additional iterative method has been conceived but has yet to be evaluated. The data from figure 4(a) are reproduced in figure 13 and dashed lines have been faired through the points. Boundary layer separation on the suction surface is indicated by a flattening of the pressure distribution near the trailing edge and is drawn as a constant C_p line. It can be observed that when the separated region is represented as a constant pressure region, the suction and pressure surface distribution appear to close at the trailing edge (100-percent chord location). That is, the pressure surface flow adjusts to the region of higher static pressure produced by the suction surface separation near the trailing edge.

A pressure distribution similar to figure 13 could be produced analytically and would thereby provide a means of establishing exit angle. The procedure would require the following steps. Input surface pressures for a boundary layer calculation are provided by an inviscid flow calculation. The location (X/C_t) of suction surface boundary layer separation is predicted by the boundary layer calculation. The value of C_p on the suction surface at the separation location (X/C_t) is extended at constant C_p to the trailing edge. The pressure surface C_p distribution is extrapolated to the trailing edge. If the suction surface and pressure surface C_p values are equal at the trailing edge station, the β_2' used in the inviscid flow calculation is the predicted value. If not, the series of calculations is repeated until pressure surface and adjusted suction surface pressures agree at the 100-percent chord location.

Comparison of analytical methods. - Several approaches have been suggested for utilizing inviscid flow and boundary layer calculation procedures to approximate real flow conditions. Particular attention has been paid to the ability to predict surface pressure distributions and outlet angle. In this section some advantages and disadvantages of each approach are enumerated to allow a comparative assessment to be made of the utility (cost) and accuracy of the suggested approaches.

One approach, yet undeveloped, would involve a correlation of the location of crossing of the suction and pressure surface pressures (and thereby the exit angle that produced it) and aerodynamic parameters available from the inviscid flow calculation and

perhaps the boundary layer calculation as well. Such a method appears feasible. It would be very simple to apply. But much data correlation would be required to develop it.

The extended Gostelow method showed a good ability to predict exit angle. Predictions of surface pressure distributions were good, but not exact. (In fig. 12 the extended Gostelow method and the displacement thickness added methods are compared, and their abilities to predict surface pressure distribution appear to be about equal.) The basic method developed by Gostelow is well documented and was shown to work well for low cambered blades (refs. 17 and 21). The extension in this report to highly cambered blades showed equally good promise. It requires several iterations to apply but consists of relatively simple operations. It retains the disadvantages of the basic method, that is, the empirical basis, and the necessity to manually fair-in tangents.

The displacement-thickness-added method predicted surface pressures with about equal accuracy as the extended Gostelow method. Predictions of fluid exit angle were acceptable. The method at present does possess some serious disadvantages, however. The assumptions for initial boundary layer thicknesses in the boundary layer calculations are crucial in this method. The initial thicknesses will determine the new profile geometry: profile thickness, local surface slopes, and trailing edge thickness. And there is little reliable information to guide the user in this choice. Furthermore, the necessity to fit a spline curve through the new effective profile coordinates is time consuming, and it must be done correctly to obtain meaningful results.

Weighing the advantages and disadvantages of each method, based on the experience gained in this study, the extended Gostelow method appears to be the more serviceable method. It demonstrates acceptable accuracy and, although several iterations are necessary to arrive at a solution, the procedures are not cumbersome.

The two iterative methods discussed showed reasonably close comparison between calculated and measured blade surface pressures (velocities). The user is therefore able to obtain a direct and reasonably accurate determination of blade surface velocity deceleration. It is interesting to note that the deceleration of blade surface velocity has previously been utilized to give a measure of the blade loading. Lieblein's D-factor (ref. 21), for example, is an attempt to calculate the velocity deceleration on the blade suction surface from the known velocity diagrams at the blade inlet and outlet stations. This D-factor was developed for near design incidence angle applications. The ability to calculate blade surface velocities (pressures) with reasonable accuracy offers a more direct method to indicate blade loading levels at all operating conditions and, therefore, to predict useful operating range.

SUMMARY OF RESULTS

Analytically computed flow parameters for the midspan, double-circular arc blade section of a highly loaded compressor stator have been compared with measured flow parameters. Analytical procedures used included calculations for inviscid flow on a blade-to-blade flow plane, for boundary layer on the blade suction and pressure surfaces, and for total pressure loss coefficient. All velocities were subsonic. Comparisons were made at three incidence angles between experimentally measured and computed blade surface pressure distributions, outlet flow angle, and loss coefficient.

Two-dimensional calculation methods proved adequate for predicting performance at the midspan location where three-dimensional effects are believed to be minimized. Radial flows cannot be considered completely absent, however, and some portion of the discrepancy between calculated and measured flows must be attributed to them.

Inviscid Flow Calculations

In order to deduce the relations between outlet flow angle and calculated flow conditions at the blade trailing edge region, the inviscid flow calculations were carried out by two methods. In the first, the pressures on the blade suction and pressure surfaces were made equal at the blade trailing edge station and the associated fluid outlet angle accepted as a result. In the second, the measured outlet flow angles were used as input and the associated calculated flow conditions in the blade trailing edge region accepted as a result. Comparison of calculated and measured data gave the following results:

1. When the exit flow angle was adjusted to make calculated suction and pressure surfaces pressures equal at the blade section trailing edge, the following observations were made:

   (a) Favorable agreement between analytical and experimental pressures was achieved over the front portions of the blade, but divergence increased toward the trailing edge where the boundary layer and separation effects are greater.

   (b) The analytical outlet angles differed significantly (as much as 10° greater turning) from measured values.

2. When the experimentally measured outlet angle was used in the inviscid flow calculations, much better agreement between experimental and analytical surface pressures was achieved, although some differences still existed in the trailing edge region. For all three incidence angle conditions the calculated suction and pressure surface pressures became equal at the 91.5 to 92.5 percent chord location (i.e., surface pressure distributions crossed inside the trailing edge).

Boundary Layer and Loss Calculations

Boundary layer and loss calculations yielded the following results:

1. Laminar boundary layer calculations predicted laminar separation to occur before transition on both blade surfaces at all incidence angles.

2. Transition to a turbulent boundary layer was forced analytically at the indicated laminar separation point, but agreement between analytical and measured losses was not achieved, even when the boundary layer thickness was allowed to increase by a factor of five.

3. All boundary layers were subsequently calculated as initially turbulent from near the blade leading edge. Calculated loss values were made from a flow model developed by Speidel which accounts for boundary layer losses to the separation point and includes an additional term to account for loss due to separation. To make calculated losses match measured losses the following had to be done:

   (a) At the design point, initial turbulent boundary layer displacement thickness had to be 0.061 centimeter and initial momentum thickness had to be 0.0435 centimeter on each blade surface. The large required values of initial thicknesses indicate the need for further application of the calculation procedure to determine its general applicability.

   (b) As incidence angle increased, the initial thickness values had to increase.

Iterative Calculations

Two methods were considered which involved iterative use of inviscid flow and boundary layer calculations. Each produced acceptable results:

1. The first method introduced a modification (accounting for separated boundary layers) to a procedure reported by Gostelow. Boundary layer and rounded trailing edge effects are approximated by neglecting calculated surface pressures near the trailing edge and fairing-in tangents to the pressure distributions at a location upstream of the trailing edge such that the tangents cross at the trailing edge station. By iterative application of this method fluid exit angle was determined quite closely and surface pressures showed good agreement with experimental data. The boundary layer calculations were used to locate the point of turbulent separation from which a tangent was faired in to the pressure distribution.

2. The second method investigated entailed adding calculated boundary layer displacement thickness to the original blade profile geometry to define a new "effective" blade shape and then recalculating inviscid flow around this new blade profile. Resulting surface pressures showed good agreement with measured data. The prediction of the

fluid exit angle was less accurate than the extended Gostelow method, and in general, the method was more cumbersome to apply.

Lewis Research Center,
National Aeronautics and Space Administration,
Cleveland, Ohio, June 29, 1973,
501-24.

APPENDIX A

SYMBOLS

C	blade chord length, cm
C_p	static pressure coefficient, $\frac{p_l - p_1}{\frac{1}{2}\rho_1 V_1^2}$
D	diffusion factor, $1 - \frac{V'_2}{V'_1} - \frac{V_{\theta 1} - V_{\theta 2}}{2\sigma V'_1}$
F	force, N
H_i	incompressible form factor (ref. 3)
i	incidence angle, i. e., angle between inlet flow direction and line tangent to blade section meanline at leading edge, deg
M	Mach number
p	static pressure, N/m^2
s	blade spacing, cm
T	blade thickness, cm
V	velocity, m/sec
y	distance from blade meanline to blade surface (fig. 14), cm
z	axial distance, cm
β	fluid angle, with respect to axial direction, deg
$\Delta\beta$	fluid turning angle, $\beta'_2 - \beta'_1$, deg
δ	deviation angle, i. e., angle between exit flow direction and line tangent to blade section meanline at trailing edge, deg
δ^*	boundary layer displacement thickness, cm
γ	blade setting angle, deg
θ	boundary layer momentum thickness, cm
ρ	fluid density, kg/m^3
σ	blade solidity, chord to spacing ratio
φ	blade camber angle, deg
$\overline{\omega}$	blade loss coefficient, ratio of total pressure loss to inlet dynamic pressure

Subscripts:

l	local
max	maximum
p	pressure
s	suction
T	total
z	axial direction
θ	tangential direction
1	inlet flow plane
2	outlet flow plane

Superscript:

	relative

APPENDIX B

DEVELOPMENT OF SPEIDEL'S LOSS MODEL

Speidel (ref. 4) followed a similar line of development as Lieblein (ref. 9) to arrive at a loss coefficient expression for unseparated flow expressed in terms of boundary layer parameters. The analysis was for incompressible flow. The resulting expression for loss coefficient (in the nomenclature of the present report) was

$$\bar{\omega} = 2 \frac{\theta_s + \theta_p}{s \cos \beta_2'} \left(\frac{\cos \beta_1'}{\cos \beta_2'} \right)^2 \tag{B1}$$

where θ_s is the momentum thickness on the suction surface at the trailing edge and θ_p is the corresponding thickness on the pressure surface.

When separation occurs, presumably on the suction surface, Speidel expressed the additional loss in terms of a hypothetical momentum thickness θ_A. The rationale used to achieve an expression for θ_A follows.

Figure 14 represents the blade thickness against distance near the trailing edge region. The thickness distribution shown is symmetrical around the mean line. Point A on the suction surface is the point of separation and the distances from the mean line to the suction and pressure surfaces at that point are y_{s_A} and y_{p_A}. Plotted below the thickness distribution plot is a representation of surface pressure against distance. The nonseparated flow case is shown in solid lines. Both surface pressures meet at the trailing edge at pressure p_H. At point A the flow separates and the static pressure remains constant to the trailing edge. It is assumed that the pressure on the pressure surface accommodates itself to the new trailing edge pressure p_A in a linear fashion. It is also assumed that main flow total pressure remains constant between A and H.

Shown in figure 15 is a plot of surface static pressure against blade thickness. The nonseparated flow case is once again shown with solid lines and the separated case indicated by dotted lines. In the latter case, it can be seen that as a condition of zero thickness (trailing edge) is approached, both pressures become equal to p_A. Shown as a cross-hatched area is the difference between the separated and nonseparated cases. This cross-hatched area corresponds to a defect of force on the blade due to the boundary layer separation, and it can be expressed as a loss of momentum.

The defect in force can be expressed as the area of the cross-hatched triangles in figure 15. On the suction surface of the mean line,

$$F_S = (p_H - p_A) \frac{1}{2} y_{S_A}$$

and on the pressure surface side,

$$F_P = (p_H - p_A) \frac{1}{2} y_{p_A}$$

The total force defect due to pressure is

$$F_T = F_S + F_P = (p_H - p_A) y_A$$

where

$$y_A = y_{S_A} + y_{p_A}$$

and

$$y_{S_A} = y_{p_A}$$

The incompressible Bernoulli equation expressed between A and H, with total pressure assumed constant, is

$$P_{TOT} = p_A + \frac{\rho}{2} W_A^2 = p_H + \frac{\rho}{2} W_H^2$$

$$p_H - p_A = \frac{\rho}{2} \left(W_A^2 - W_H^2 \right)$$

so that now

$$F_T = \frac{\rho}{2} W_A^2 - W_H^2 \, y_A$$

The defect in momentum created by separation can be expressed in terms of a momentum thickness θ_A:

$$\text{Defect in momentum} = \rho \theta_A W_2^2$$

where W_2 is the average velocity in the outlet plane. The defect in momentum is equivalent to the total force defect, that is,

$$F_T = \rho\theta_A W_2^2$$

Substituting for F_T gives

$$\frac{\rho}{2}\left(W_A^2 - W_H^2\right)y_A = \rho\theta_A W_2^2$$

$$\theta_A = \frac{y_A}{2}\left[\left(\frac{W_A}{W_2}\right)^2 - \left(\frac{W_H}{W_2}\right)^2\right]$$

Speidel reports that experimental measurements in the region of the trailing edge show

$$\left(\frac{W_H}{W_2}\right)^2 = 0.9$$

so that

$$\theta_A = \frac{y_A}{2}\left[\left(\frac{W_A}{W_2}\right)^2 - 0.9\right]$$

The expression for loss coefficient when separation has occurred is then

$$\overline{\omega} = 2\,\frac{2(\theta_S + \theta_P + \theta_A)}{s\cos\beta_2'}\left(\frac{\cos\beta_1'}{\cos\beta_2'}\right)^2 \qquad \text{(B2)}$$

where θ_S is now the momentum thickness at the point of separation and θ_P is the momentum thickness at the trailing edge.

REFERENCES

1. Brent, J. A.: Single-Stage Experimental Evaluation of Tandem-Airfoil Rotor and Stator Blading for Compressors. Part II - Data and Performance for Stage A. Rep. PWA-FR-4719, Pratt & Whitney Aircraft (NASA CR-120804), July 1972.

2. Katsanis, Theodore: Fortran Program for Calculating Transonic Velocities on a Blade-to-Blade Stream Surface of a Turbomachine. NASA TN D-5427, 1969.

3. McNally, William D.: Fortran Program for Calculating Compressible Laminar and Turbulent Boundary Layers in Arbitrary Pressure Gradients. NASA TN D-5681, 1970.

4. Speidel, L.: Berechnung der Strömungsverluste von ungestaffelten ebenen Schaufelgittern. Dissertation, T. H. Braunschweig, 1953; Ing.-Archiv, vol. 22, 1954, pp. 295-322.

5. Cohen, Clarence B.; and Reshotko, Eli: The Compressible Laminar Boundary Layer with Heat Transfer and Arbitrary Pressure Gradient. NACA TR 1294, 1956.

6. Schlichting, Hermann (J. Kestin, trans.): Boundary Layer Theory. Sixth ed., McGraw-Hill Book Co., Inc., 1968, Ch. 22.

7. Sasman, Philip K.; and Cresci, Robert J.: Compressible Turbulent Boundary Layer with Pressure Gradient and Heat Transfer. AIAA J., vol. 4, no. 1, Jan. 1966, pp. 19-25.

8. Schlichting, H.: Application of Boundary-Layer Theory in Turbomachinery. J. Basic Eng., vol. 81, no. 4, Dec. 1959, pp. 543-551.

9. Walker, G.: The Prediction of Boundary Layer Development on Axial Flow Turbomachine Blades. Proceedings of the Third Australian Conference on Hydraulics and Fluid Mechanics. Institution of Engineers, Australia, 1968, pp. 97-104.

10. Sandborn, V. A.; and Liu, C. Y.: On Turbulent Boundary-Layer Separation. J. Fluid Mech., vol. 32, pt. 2, May 3, 1968, pp. 293-304.

11. Cockrell, D.; Hill, P.; Lumley, J.; Morkovin, M.; and Emmons, H.: Report of Evaluation Committee. Computation of Turbulent Boundary Layers. Vol. 1. AFOSR-IFP Stanford Univ., 1969, pp. 464-478.

12. von Doenhoff, A. E.; and Tetervin, N.: Determination of General Relations for the Behavior of Turbulent Boundary Layers. NACA Wartime Rep. L-382, 1943.

13. Lieblein, Seymour; and Roudebush, William H.: Theoretical Loss Relations for Low-Speed Two-Dimensional Cascade Flow. NACA TN 3662, 1956.

14. Stewart, Warner L.: Analysis of Two-Dimensional Compressible-Flow Loss Characteristics Downstream of Turbomachine Blade Rows in Terms of Basic Boundary-Layer Characteristics. NACA TN 3515, 1955.

15. Brent, J. A.; Cheatham, J. G.; and Nilsen, A. W.: Single-Stage Experimental Evaluation of Tandem-Airfoil Rotor and Stator Blading for Compressors. Part I - Analysis and Design of Stages A, B, and C. Rep. PWA-FR-4667, Pratt & Whitney Aircraft (NASA CR-120803), June 1972.

16. Johnsen, Irving A.; and Bullock, Robert O.; eds.: Aerodynamic Design of Axial-Flow Compressors. NASA SP-36, 1965.

17. Gostelow, J. P.: The Accurate Prediction of Cascade Performance. Thesis, Liverpool Univ., Sept. 1965.

18. Becker, John V.: Boundary-Layer Transition of the NACA 0012 and 23012 Airfoils in the 8-Foot High-Speed Wind Tunnel. NACA Wartime Rep. L-682, 1940.

19. Preston, J. H.: The Calculation of Lift Taking Account of the Boundary Layer. R&M 2725, Aeronautical Res. Council, Gt. Britain, 1953.

20. Spence, D. A.; and Beasley, J. A.: The Calculation of Lift Slopes, Allowing for Boundary Layer, with Application to the RAE 101 and 104 Aerofoils. R&M 3137, Aeronautical Res. Council, Gt. Britain, 1960.

21. Miller, Max J.: Some Aspects of Deviation Angle Estimation for Axial-Flow Compressors. Thesis, Iowa State Univ., 1973.

22. Lieblein, Seymour; Schwenk, Francis C.; and Broderick, Robert L.: Diffusion Factor for Estimating Losses and Limiting Blade Loadings in Axial-Flow-Compressor Blade Elements. NACA RM E53D01, 1953.

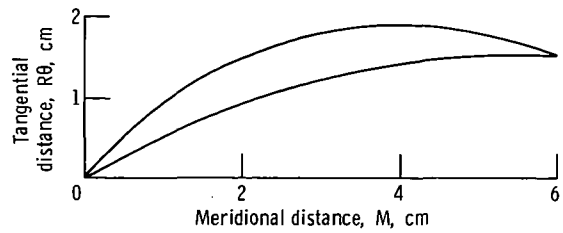

Figure 1. - Stator blade section geometry at midspan section.

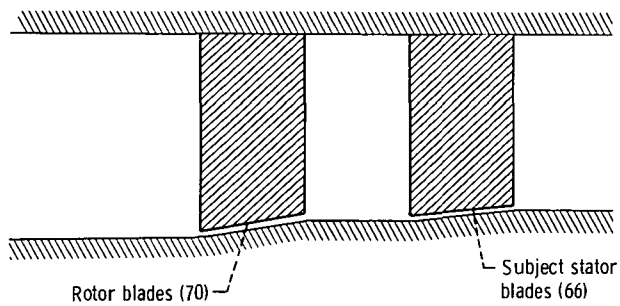

Figure 2. - Cross section of flow path showing lack of curvature.

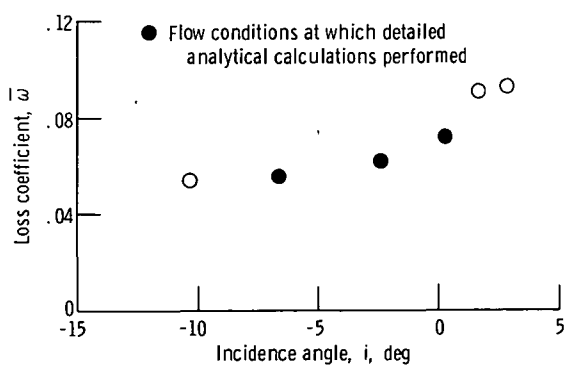

Figure 3. - Stator experimental loss coefficient at mid-span section.

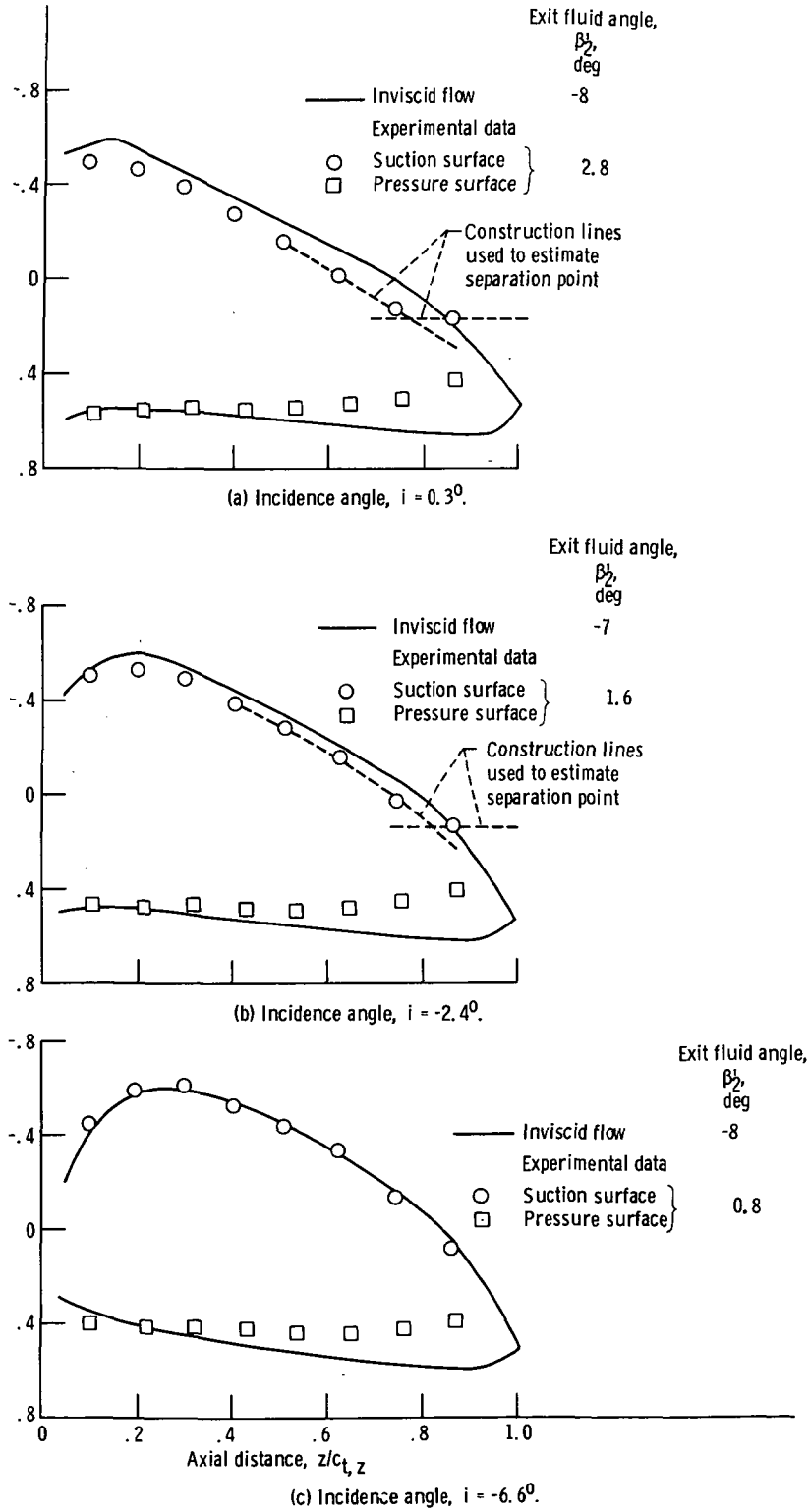

Figure 4. - Comparison of experimental and analytical surface pressure coefficients. Closure at trailing edge.

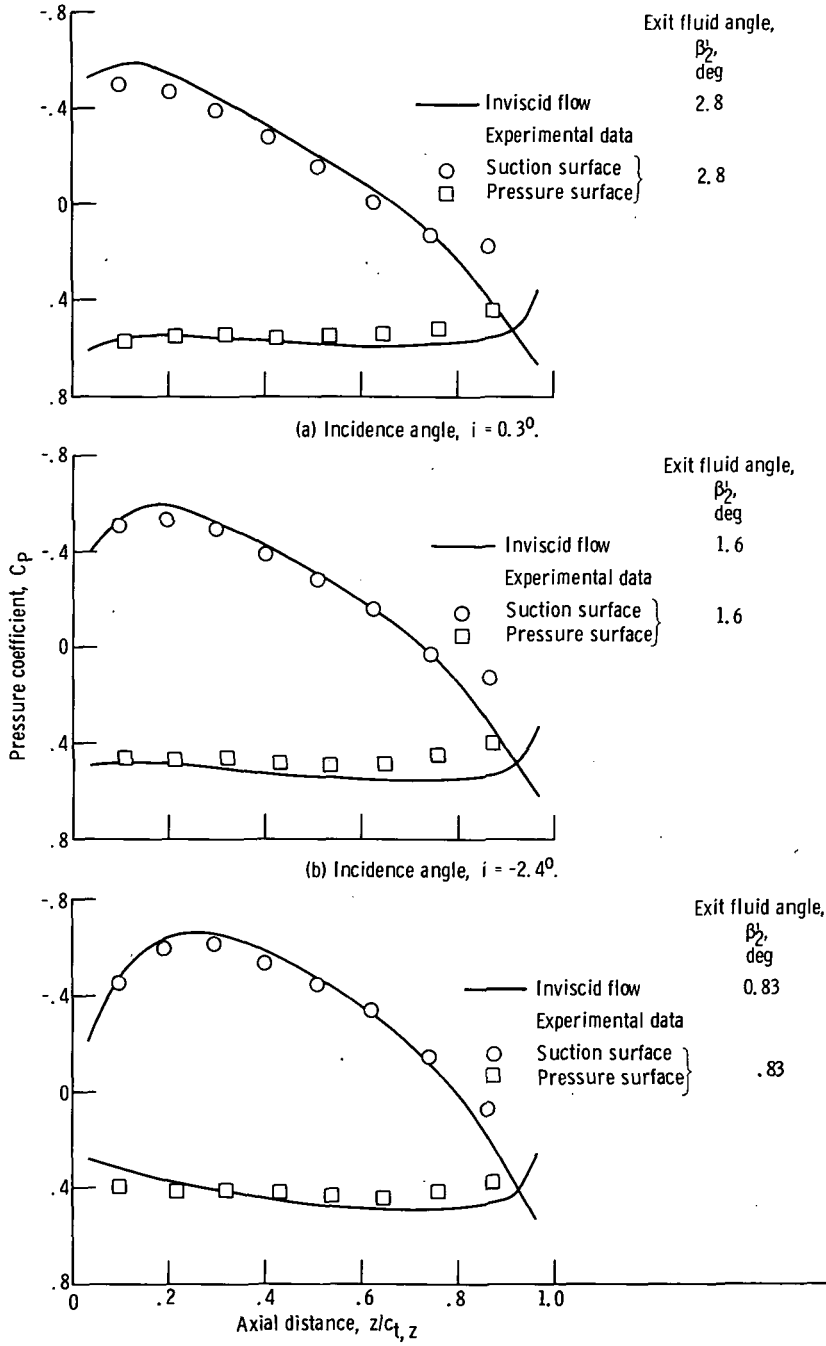

Figure 5. - Comparison of experimental and analytical surface pressure coefficients. Experimental exit angle used in analytical calculations.

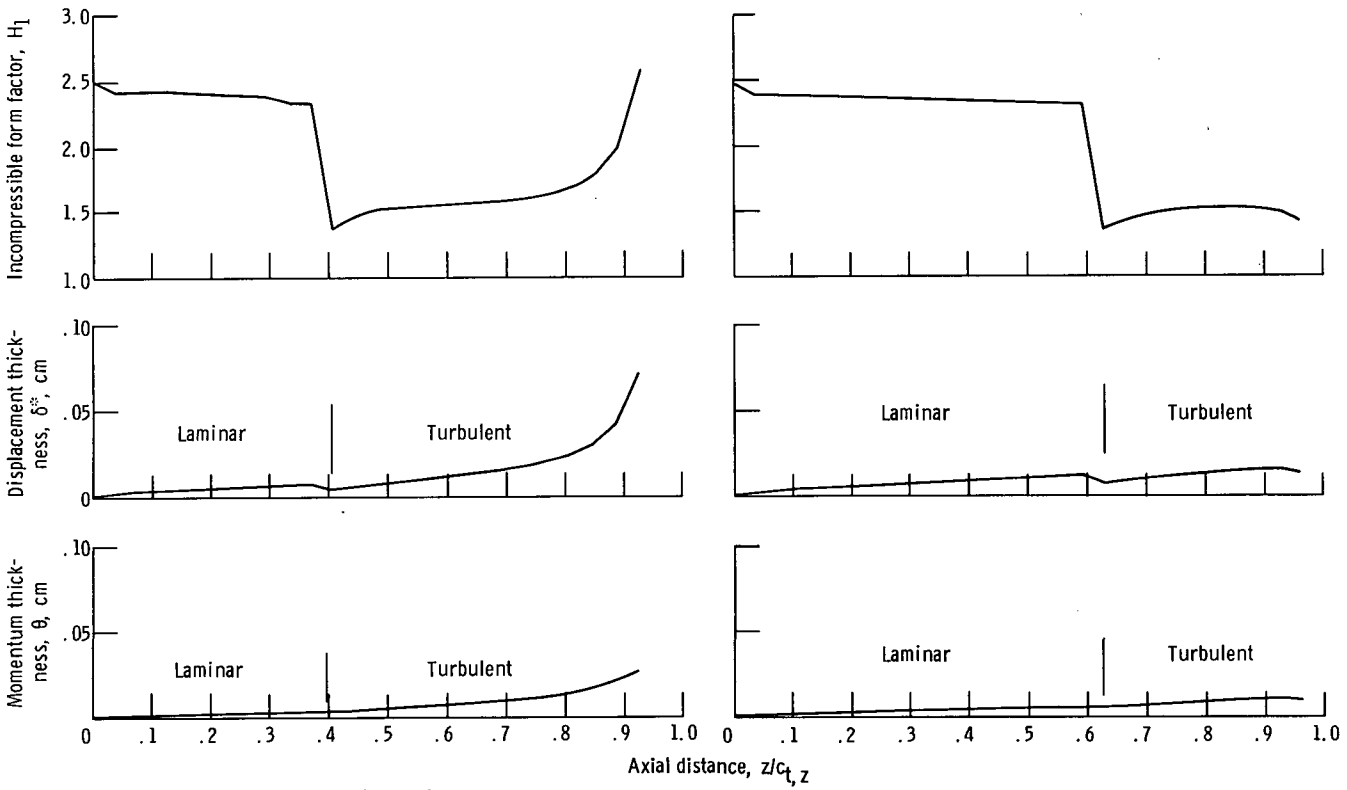

(a) Suction surfaces.

(b) Pressure surfaces.

Figure 6. - Boundary layer development with initially laminar boundary. Incidence angle, i = -2.405.

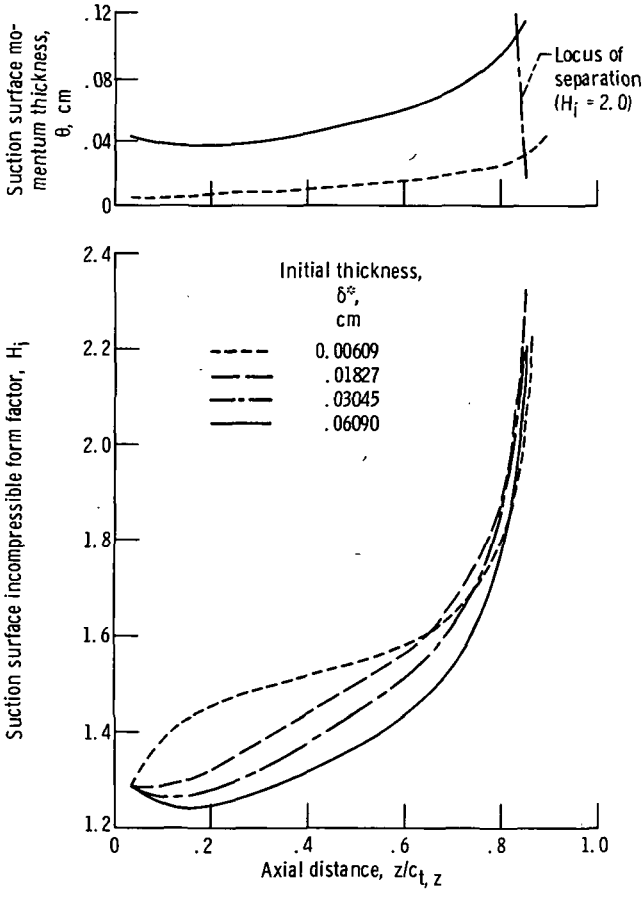

Figure 7. - Effect of initial turbulent boundary layer thickness on incompressible form factor and momentum thickness. Analytical pressure distribution; design incidence, $i = -2.405^0$.

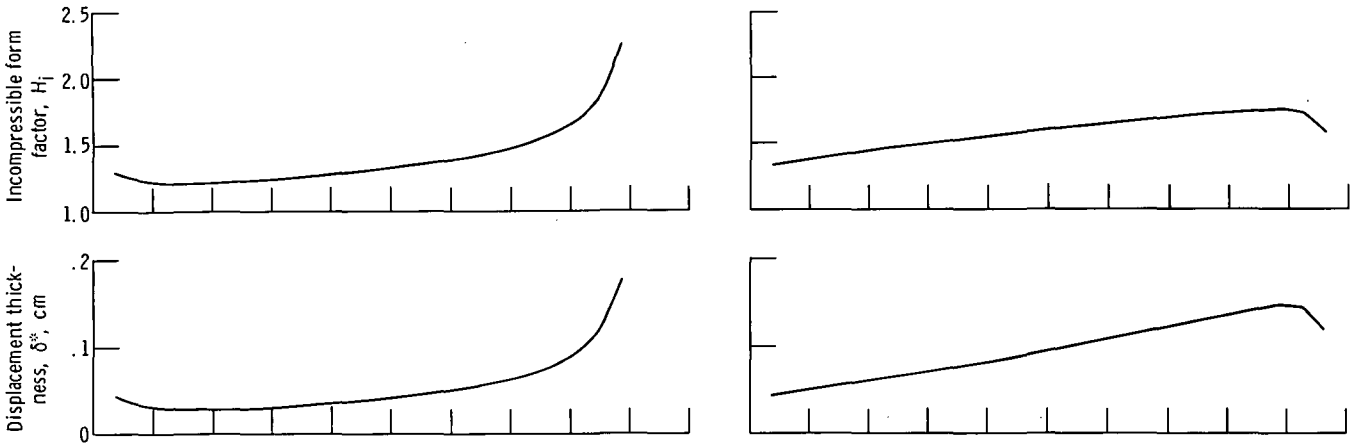

(a-1) Suction surfaces.

(a-2) Pressure surfaces.

(a) Incidence angle, $i = -6.6^0$.

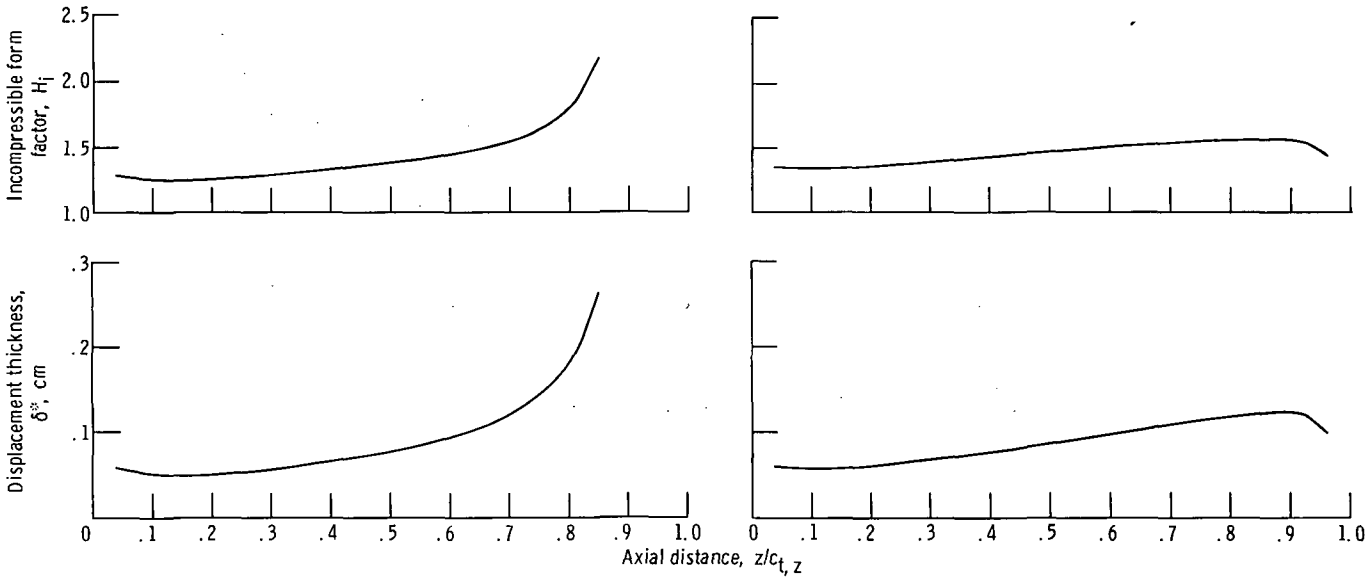

(b-1) Suction surfaces.

(b-2) Pressure surfaces.

(b) Incidence angle, $i = -2.4^0$.

Figure 8. - Boundary layer development with initially turbulent boundary layer.

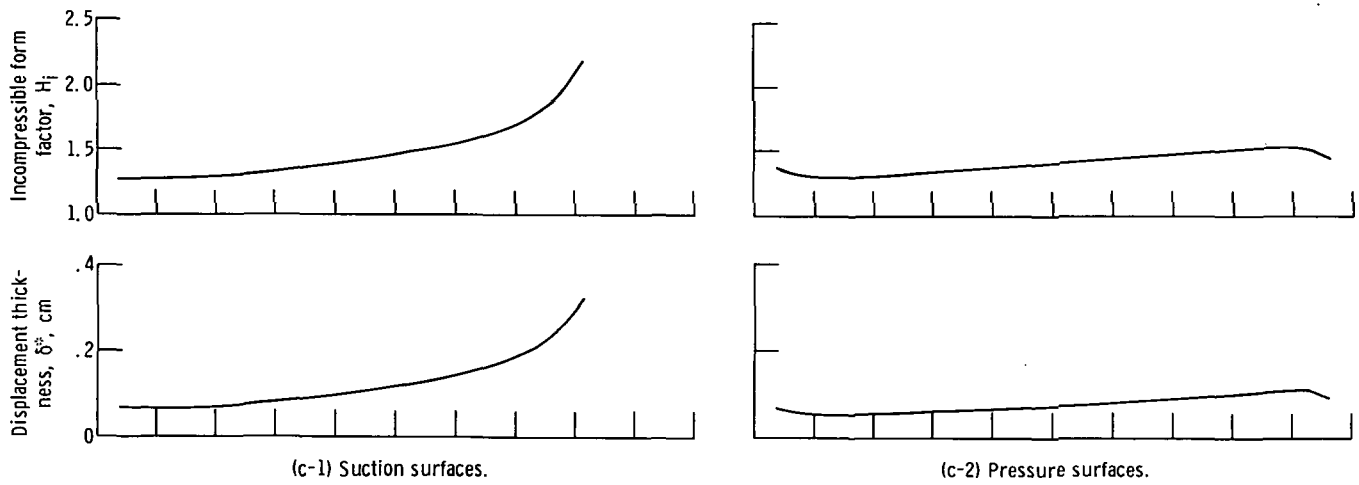

(c-1) Suction surfaces.

(c-2) Pressure surfaces.

(c) Incidence angle, $i = 0.3^0$.

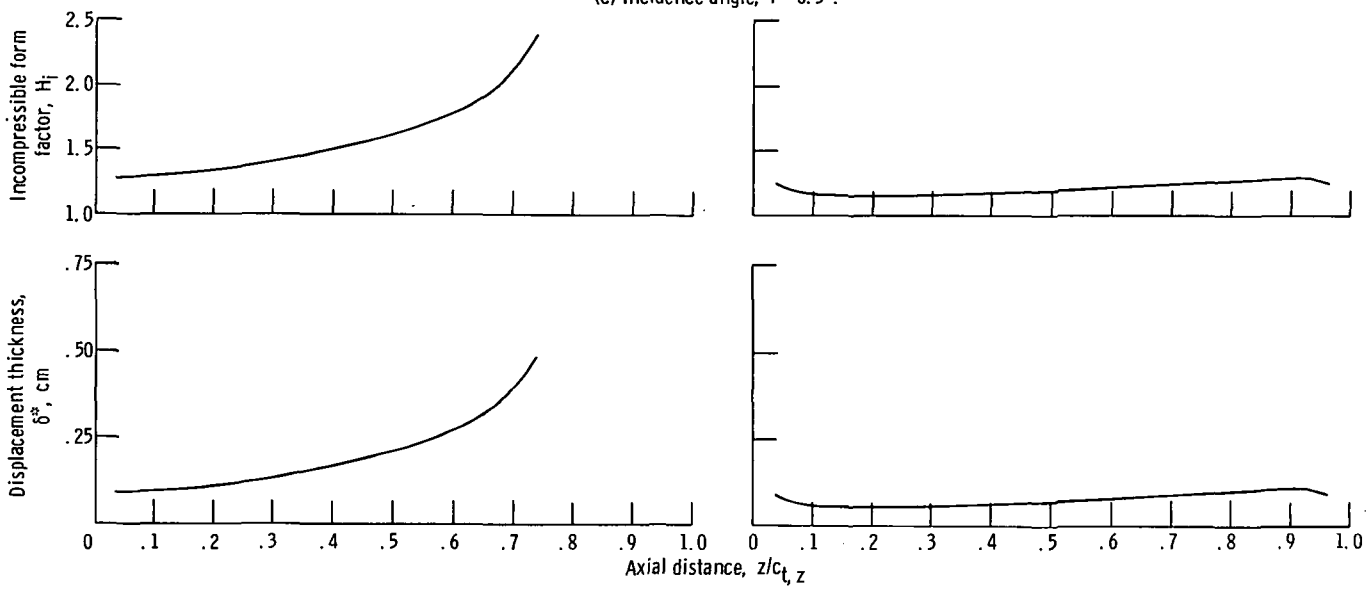

(d-1) Suction surfaces.

(d-2) Pressure surfaces.

(d) Incidence angle, $i = 2.9^0$.

Figure 8. - Concluded.

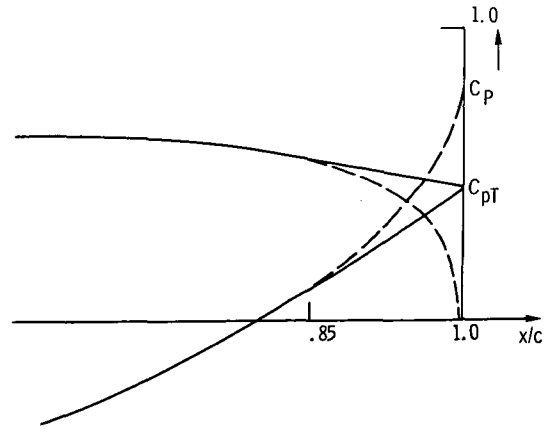

Figure 9. - Illustration of "fairing-in" process (from Gostelow, ref. 17).

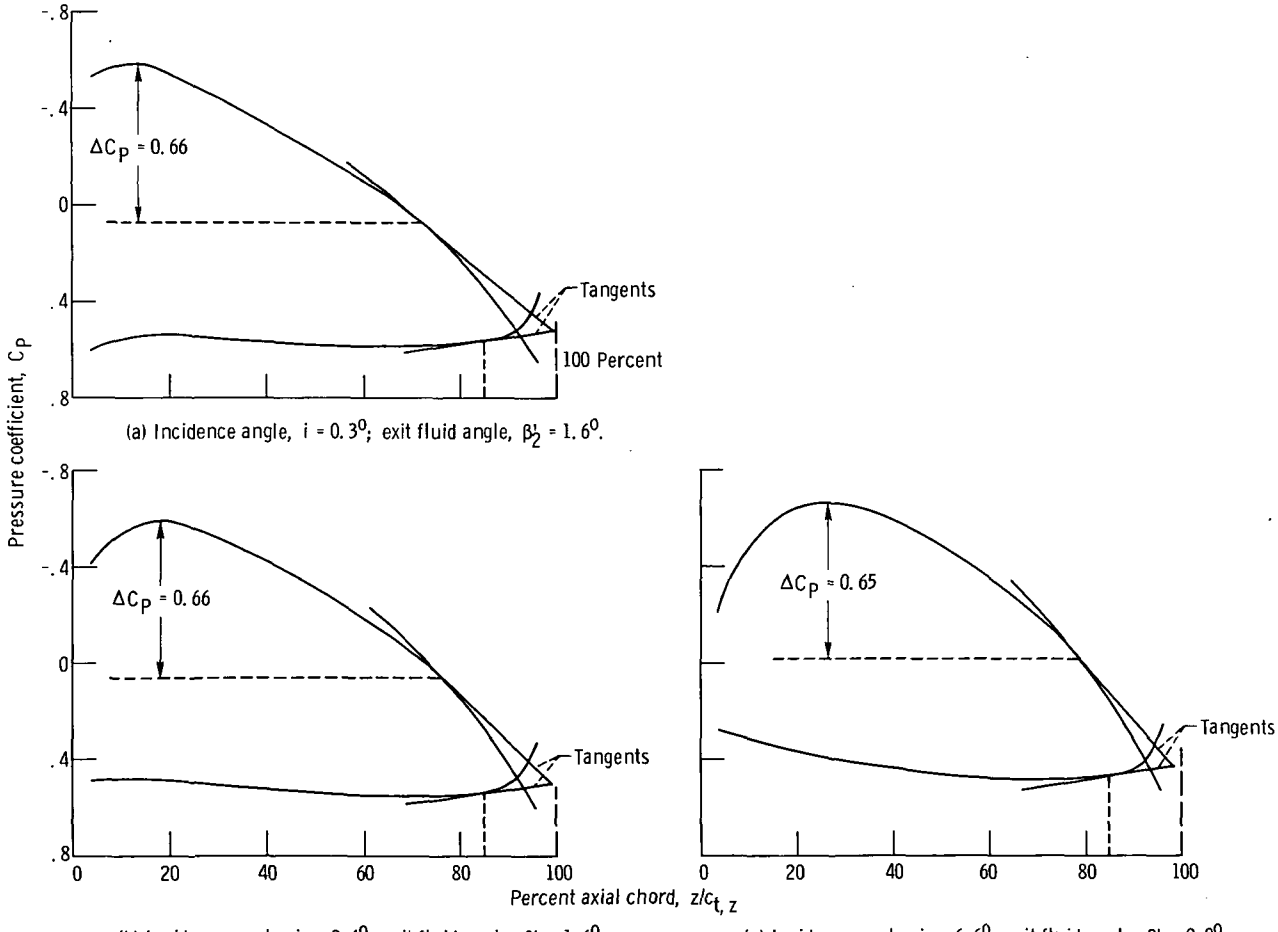

(a) Incidence angle, $i = 0.3^0$; exit fluid angle, $\beta_2' = 1.6^0$.

(b) Incidence angle, $i = -2.4^0$; exit fluid angle, $\beta_2' = 1.6^0$.

(c) Incidence angle, $i = -6.6^0$; exit fluid angle, $\beta_2' = 0.8^0$.

Figure 10. - Extended Gostelow method using faired-in tangents in trailing-edge region.

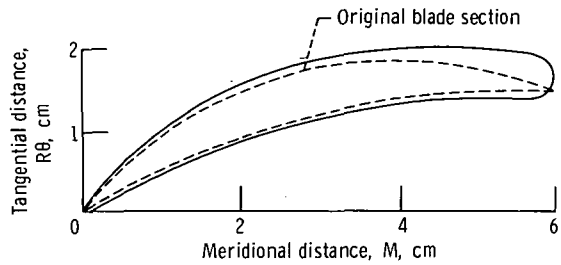

Figure 11. - Stator blade section with boundary layer displacement thickness added.

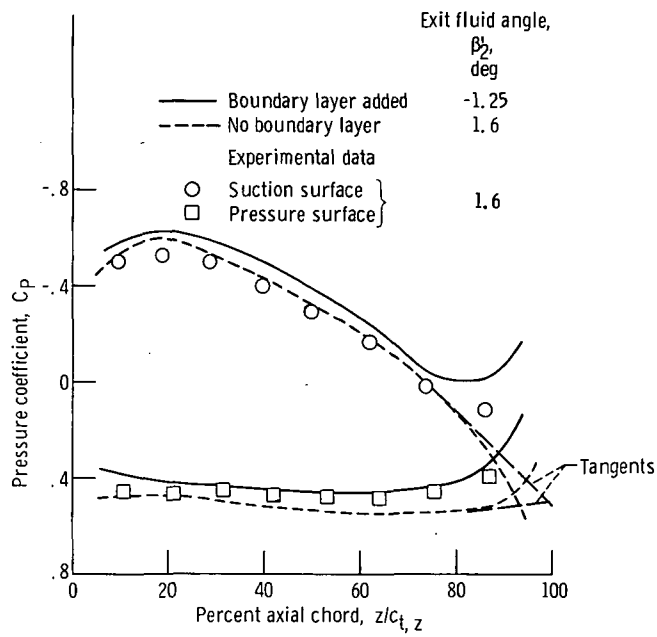

Figure 12. - Comparison of experimental and analytical surface pressure coefficients. Corrected and uncorrected for boundary layer design point, $i = -2.4^{\circ}$.

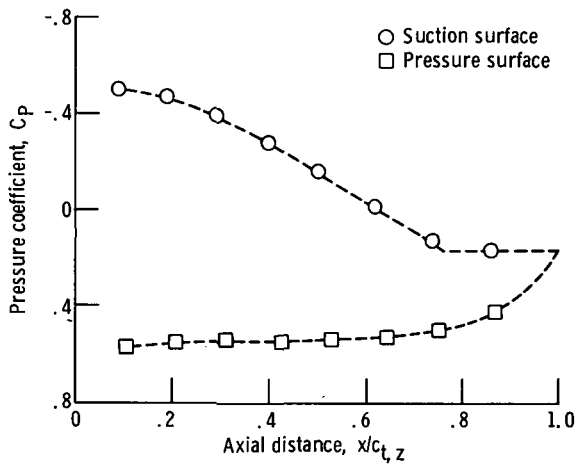

Figure 13. - Experimental surface pressure coefficients showing effect of boundary layer separation on trailing edge closure condition. Incidence angle, $i = 0.3^{\circ}$.

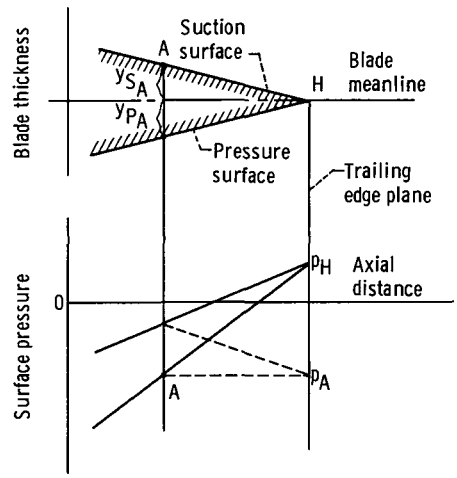

Figure 14. - Schematic of trailing edge blade profile and pressure distribution with and without boundary layer separation.

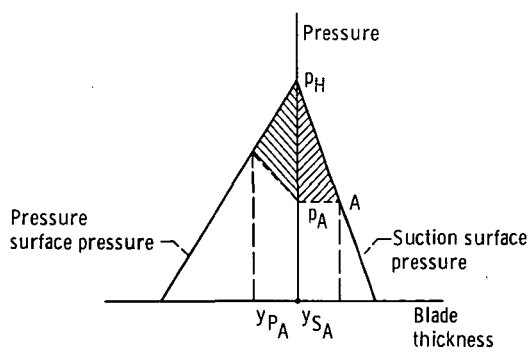

Figure 15. - Schematic of pressure defect due to boundary layer separation.

NASA-Langley, 1973 —— 1 E-7280

NATIONAL AERONAUTICS AND SPACE ADMINISTRATION
WASHINGTON, D.C. 20546

OFFICIAL BUSINESS
PENALTY FOR PRIVATE USE $300

SPECIAL FOURTH-CLASS RATE BOOK

POSTAGE AND FEES PAID
NATIONAL AERONAUTICS AND SPACE ADMINISTRATION
451

U.S.MAIL

POSTMASTER: If Undeliverable (Section 158 Postal Manual) Do Not Return

"The aeronautical and space activities of the United States shall be conducted so as to contribute . . . to the expansion of human knowledge of phenomena in the atmosphere and space. The Administration shall provide for the widest practicable and appropriate dissemination of information concerning its activities and the results thereof."

—NATIONAL AERONAUTICS AND SPACE ACT OF 1958

NASA SCIENTIFIC AND TECHNICAL PUBLICATIONS

TECHNICAL REPORTS: Scientific and technical information considered important, complete, and a lasting contribution to existing knowledge.

TECHNICAL NOTES: Information less broad in scope but nevertheless of importance as a contribution to existing knowledge.

TECHNICAL MEMORANDUMS: Information receiving limited distribution because of preliminary data, security classification, or other reasons. Also includes conference proceedings with either limited or unlimited distribution.

CONTRACTOR REPORTS: Scientific and technical information generated under a NASA contract or grant and considered an important contribution to existing knowledge.

TECHNICAL TRANSLATIONS: Information published in a foreign language considered to merit NASA distribution in English.

SPECIAL PUBLICATIONS: Information derived from or of value to NASA activities. Publications include final reports of major projects, monographs, data compilations, handbooks, sourcebooks, and special bibliographies.

TECHNOLOGY UTILIZATION PUBLICATIONS: Information on technology used by NASA that may be of particular interest in commercial and other non-aerospace applications. Publications include Tech Briefs, Technology Utilization Reports and Technology Surveys.

Details on the availability of these publications may be obtained from:

SCIENTIFIC AND TECHNICAL INFORMATION OFFICE

NATIONAL AERONAUTICS AND SPACE ADMINISTRATION

Washington, D.C. 20546